EUROPEAN HEMATOLOGY ASSOCIATION
haematologica
Journal of the European Hematology Association

Depletion of SIRT6 enzymatic activity increases acute myeloid leukemia cells vulnerability to DNA-damaging agents

by Antonia Cagnetta, Debora Soncini, Stefania Orecchioni, Giovanna Talarico, Paola Minetto, Fabio Guolo, Veronica Retali, Nicoletta Colombo, Enrico Carminati, Marino Clavio, Maurizio Miglino, Micaela Bergamaschi, Aimable Nahimana, Michael Duchosal, Katia Todoerti, Antonino Neri, Mario Passalacqua, Santina Bruzzone, Alessio Nencioni, Francesco Bertolini, Marco Gobbi, Roberto M. Lemoli, and Michele Cea

Haematologica 2017 [Epub ahead of print]

Citation: Cagnetta A, Soncini D, Orecchioni S, Talarico G, Minetto P, Guolo F, Retali V, Colombo N, Carminati E, Clavio M, Miglino M, Bergamaschi M, Nahimana A, Duchosal M, Todoerti K, Neri A, Passalacqua M, Bruzzone S, Nencioni A, Bertolini F, Gobbi M, Lemoli RM, and Cea M. Depletion of SIRT6 enzymatic activity increases acute myeloid leukemia cells vulnerability to DNA-damaging agents. Haematologica. 2017; 102:xxx
doi:10.3324/haematol.2017.176248

Depletion of SIRT6 enzymatic activity increases acute myeloid leukemia cells vulnerability to DNA-damaging agents

Antonia Cagnetta [1,2*], Debora Soncini [1*], Stefania Orecchioni [3], Giovanna Talarico [3], Paola Minetto [1], Fabio Guolo [1], Veronica Retali [1,2], Nicoletta Colombo [1], Enrico Carminati [1], Marino Clavio [1,2], Maurizio Miglino [1,2], Micaela Bergamaschi [1], Aimable Nahimana [4], Michel Duchosal [4], Katia Todoerti [5], Antonino Neri [6,7], Mario Passalacqua [8], Santina Bruzzone [8], Alessio Nencioni [2,9], Francesco Bertolini [3], Marco Gobbi [1,2], Roberto M. Lemoli [1,2**] and Michele Cea [1,2**]

[1]Chair of Hematology, Department of Internal Medicine (DiMI), University of Genoa. Genova, Italy.
[2] Hematology Unit, Policlinico San Martino. Genova, Italy.
[3] European Institute of Oncology. Milan, Italy.
[4]Service and Central Laboratory of Hematology, University Hospital of Lausanne. Lausanne, Switzerland.
[5]Laboratory of Pre-Clinical and Translational Research, IRCCS-CROB, Referral Cancer Center of Basilicata. Rionero in Vulture, Potenza, Italy
[6]Department of Oncology and Hemato-Oncology, University of Milan. Milan , Italy
[7]Hematology Unit, Fondazione Cà Granda, Ospedale Maggiore Policlinico. Milan, Italy
[8]Department of Experimental Medicine, University of Genoa. Genoa, Italy.
[9] Department of Internal Medicine, University of Genoa. Genoa, Italy.

*A.C. and D.S. are co-first authors
**M.C and R.M.L. are co-senior authors

Running head: SIRT6 inhibition increases anti-leukemic activity of chemotherapy

Address correspondence and request for reprints: Michele Cea, M.D., Department of Internal Medicine and Specialities (DiMI), University of Genoa, 16132 Genoa, Italy. Phone: 39-010-353-7970; Fax: 39-010-353-7989; E-mail: michele.cea@unige.it

Abstract word count: 189

Main text word count: 3,927

Figures: 7

Supplemental file: 1

Acknowledgments

The authors thank Dr. Barbara Parodi and Dr. Paola Visconti (Bio banking core facility at IRCCS AOU san Martino Hospital, Genoa) for providing AML cell lines. In addition we thank all clinicians for their helpful suggestions. This work was supported in part by the Associazione Italiana per la Ricerca sul Cancro (AIRC, My First Grant #18491, to M.C.), Italian Ministry of Health (5 x 1000 Funds of IRCCS San Martino-IST 2014, to M.C.), Associazione Italiana Leucemie & Società Italiana di Ematologia Sperimentale fellowship (AIL-SIES, to D.S.) and University of Genoa, Italy.

ABSTRACT

Genomic instability plays a pathological role in various malignancies, including acute myeloid leukemia, and thus represents potential therapeutic target. Recent studies demonstrate that SIRT6, a NAD+-dependent nuclear deacetylase, functions as genome-guardian by preserving DNA integrity in different tumor cells. Here, we demonstrate that also $CD34^+$ blasts from Acute Myeloid Leukemia patients show ongoing DNA damage and SIRT6 overexpression. Indeed, we identified a poor-prognostic subset of patients, with widespread instability, which relies on SIRT6 to compensate for DNA-replication stress. As result, SIRT6 depletion compromises the ability of leukemia cells to repair DNA double-strand breaks that, in turn, increases their sensitivity to daunorubicin and Ara-C, both in vitro and in vivo. In contrast, low SIRT6 levels observed in normal $CD34^+$ hematopoietic progenitors explain their weaker sensitivity to genotoxic stress. Intriguingly, we have identified DNA-PKcs and CtIP deacetylation as crucial for SIRT6-mediated DNA repair. Together, our data suggest that inactivation of SIRT6 in leukemia cells leads to DNA-repair mechanisms disruption, genomic instability and aggressive Acute Myeloid Leukemia. This synthetic lethal approach, enhancing DNA damage while concomitantly blocking repair responses, provides the rationale for the clinical evaluation of SIRT6 modulators in leukemia treatment.

INTRODUCTION

Acute myeloid leukemia (AML) is an aggressive form of cancer with an estimated incidence in Europe of three to five cases per 100.000 people. (1, 2) It is a highly heterogeneous disease, both biologically and clinically, with variable prognosis. Despite the improvement in our understanding of the biology of AML, treatment outcome has not improved in the past 20 years. (3, 4) Chemotherapy remains the backbone of therapy whereas stem cell transplantation is mainly offered to young patients (age< 60 years). (5, 6) Therefore, the majority of AML patients (e.g. elderly patients), who are often unable to tolerate intensive treatments, face a particularly poor prognosis. (7) Thus, there is an urgent need to overcome biologic mechanisms underlying drug resistance in AML, to enhance the efficacy of existing treatments and to facilitate the design of novel approaches. Several studies show that AML oncogenes, such as MLL fusions, N-RAS, and FLT3-ITD, by promoting replication and oxidative stress, can lead to DNA damage accumulation. (8-12) In these cases, upregulation of DNA damage response (DDR) provides AML cells with a selective survival advantage, but also creates room for synthetic lethal interventions.

Sirtuins are a family of NAD^+-dependent deacetylase modifying enzymes that are upregulated in a wide range of tumors and have a central role in integrating growth signals that regulate a number of cellular pathways including metabolism, genome stability, cell proliferation, and survival. (13, 14) Recently, we have demonstrated that Multiple Myeloma (MM) cells exhibit constitutive overexpression of SIRT6, a member of this family with a critical role for DNA damage repair, which provides implications for both tumorigenesis and treatment of this tumor. (15) Here, we show that SIRT6 has biological relevance also in AML being frequently upregulated in tumor cells compared with normal $CD34^+$ hematopoietic progenitors. Importantly, such feature is associated with a signature of chromosomal instability (CIN) which in turn confers poor prognosis to a subgroup of AML patients.(16) Consistent with its observed role, SIRT6 loss unleashes genomic instability thus

triggering hypersensitivity to clinically used DNA-damaging agents, including daunorubicin (DNR) and cytarabine (ARA-C), both in-vitro and in-vivo. Mechanistically, SIRT6 binds DNA damage sites, recruits and activates, by deacetylation, DNA-PKcs and CtIP promoting overall DNA repair.

Altogether, our findings suggest that hematologic cancers, including AML, have constitutive ongoing DNA damage as well as DNA repair response steadily activated. As a result, strategies aimed to shift the balance towards high DNA damage and reduced DNA repair by SIRT6 inhibition can decrease tumor growth and may benefit patients with otherwise unfavorable outcomes.

METHODS

For a more detailed description of the methods used, see supplemental experimental procedures.

Cell lines and Reagents

The AML cell lines U937, MOLM-14, MV4-11, HL60, HEL, THP-1, NOMO-1, OCI-AML2, OCI-AML3 and NB4 were provided by collaborators or purchased from ATCC or DSMZ (Braunschweig, Germany). All cell lines were cultured in RPMI-1640 medium containing 10% FBS (GIBCO, Life Technologies, Carlsbad, CA), 2 μM l−1 glutamine, 100 U ml−1 penicillin, and 100 μg ml−1 streptomycin (GIBCO, Life Technologies, Carlsbad, CA). 293T cell line was purchased from ATCC and cultured in DMEM containing 10% FBS (GIBCO, Life Technologies, Carlsbad, CA), 2 μM l−1 glutamine, 100 U ml−1 penicillin, and 100 μg ml−1 streptomycin (GIBCO, Life Technologies, Carlsbad, CA). Daunorubicin (DNR) and cytarabine (ARA-C) were purchased from Selleck Chemicals LLC (Houston, TX) and Sigma-Aldrich (St.Louis, MO), respectively; SIRT6 chemical inhibitor (2,4-dioxo-N-(4-(pyridin-3-yloxy)phenyl)-1,2,3,4-tetrahydroquinazoline-6-sulfonamide, henceforth named compound 1) was obtained from MolPort (Riga, Latvia).

Primary cell isolation from patient samples

All studies involving human samples were performed under IRCCS AOU San Martino Hospital (Genoa, Italy) IRB committee-approved protocols, after informed consent; de-identified samples were utilized. Patient AML cells (n=20) were obtained from bone marrow samples with high disease load (>90% $CD34^+$ blasts in the marrow) and mononuclear cells were isolated by Ficoll-Hypaque gradient separation as described previously.(17) Normal mononuclear cells (MNCs) were isolated from BM healthy donors by Ficoll-Hypaque centrifugation. In some experiments, normal PB MNCs were processed by MiniMacs high-gradient magnetic separation column (Miltenyi Biotec, Bergisch Gladbach, Germany) to obtain highly purified CD34+ cells. Cells were either used immediately for

viability assays or for mRNA isolation, or stored at −80°C in medium containing 50% FBS and 10% DMSO.

Statistical analyses

All data are shown as means±SD. The Student's t test was used to compare two experimental groups using Graph-Pad Prism software. Correlation of SIRT6 expression with disease progression and OS was measured using the Kaplan-Meier method, with log-rank test for group comparison. Significance was $p< 0.05$.

RESULTS

SIRT6 is consistently overexpressed in CD34$^+$ blasts of AML patients

SIRT6 is a chromatin remodeling-deacetylase involved in tumorigenesis. (15, 18-21) In order to explore its function in AML, we tested a panel of leukemia cell lines and patient-derived tumor cells to evaluate presence of this protein. All tested tumor cells showed higher SIRT6 staining than normal cells, regardless of their genetic landscape. (Fig.1A) Notably, immunofluorescence analysis of selected AML cell lines (Fig.1B) confirmed a prominent, although not restricted, nuclear localization of this protein, as already reported in different tumors. (15, 22-24) Next, SIRT6 expression was further analyzed by querying publicly available data sets. (25, 26) Significant higher SIRT6 mRNA level was found in tumor samples (n=300) compared with PB and BM normal hematopoietic and stem cells, including CD34$^+$ stem/progenitor cells (HSPCs), more primitive CD34+ CD38- cells and unselected mononuclear cells (from BM or PB). (Fig.1C) Correlative analysis of SIRT6 levels with clinic-pathological features suggested significant association between SIRT6 expression and French-American-British (FAB) classification. (Fig. S1A) Indeed, among AML groups SIRT6 was higher in FAB M0 and M5 whilst FAB M6 subgroup was enriched in patients with SIRT6 low levels. The increased SIRT6 expression in tumors vs normal controls was further verified by performing a similar analysis on primary CD34$^+$ blast cells obtained from AML patients (n=200) collected at our Hematologic unit, compared with bone marrow as well as peripheral blood mononuclear cells (PBMCs) from healthy donors (n=10). (Fig.1D) A subsequent investigation focused on molecular features showed that SIRT6 high levels were significantly censured in FLT3-ITD mutant than in FLT3 wild-type (p=0.034), otherwise no correlations were observed between SIRT6 expression and further abnormalities including NPM1, BAALC and WT1. (Fig. S1B) Among these 200 AML patients, detailed survival information was available for 100 cases. As a result, we retrospectively analyzed the prognostic significance of baseline SIRT6 expression from BM aspirate samples on the overall

survival. Results show a statistically significant inverse correlation between SIRT6 levels and overall survival, with high SIRT6 expression associated with shorter survival rates than low expression (median survival 16 vs 32 months, p=.025). (Fig.1 E) These results were also observed by analyzing other publicly available AML patient data sets, (27) which confirmed the higher SIRT6 expression in tumors as well as its prognostic significance. (Fig.S2 A,B) Together, our data suggest a role of SIRT6 in the pathogenesis of AML providing also a rationale for its targeting.

SIRT6 controls AML cells proliferation and makes them vulnerable to DNA-Damage Agents.

To further elucidate the possible oncogenic role of SIRT6 in AML, we investigated the effect of its genetic depletion by employing a lentiviral-mediated long-term gene knockdown with two shRNA constructs targeting SIRT6. (Fig.2A) We chose two AML cell lines with robust SIRT6 expression and the role of SIRT6 in cell viability and proliferation was assessed. Surprisingly, introduction of SIRT6-targeted shRNA induced significant increase in cell numbers and cell-cycle progression, that were proportional to the reduction in protein levels (Fig.2A-B); instead SIRT6 overexpression did not affect cell count, due to the high SIRT6 levels at baseline (data not shown). These findings, as already observed in MM and in various solid tumors are likely to account for the discrepancies in the tumor burden, but clearly contrast with SIRT6 overexpression in AML patients.(15, 28) Such paradoxical behavior prompted us to hypothesize a tumor-specific role for this NAD^+-dependent histone deacetylase.

As SIRT6 has been found to play a key role in mediating DNA repair mechanisms, (22, 29-32) we investigated whether it acts as genome-guardian also in AML blasts. SIRT6 depleted cell lysates subjected to western blot analysis, showed an increased γ-H2A.X staining, suggesting that downregulation of SIRT6 expression enhances instability of AML cells. (Fig. 2C and S3) Importantly, these changes were not associated with DNA response activation, since pATM, pATR, pCHK1 and pCHK2 were almost unchanged after SIRT6 silencing. Similarly, replicative stress markers, including

RAD51, resulted unaffected by gene-knockdown in AML cells. (Fig. 2C and S3) Overall these data indicate that SIRT6 depletion freezes DNA repair mechanisms which in turn lead to greater damage. Lack of DNA repair efficiency sensitizes cancer cells to DNA damaging agents (DDAs). (33) Based on the observation that SIRT6 affects such mechanisms in AML, we hypothesized that cells depleted of SIRT6 would be more sensitive to the genotoxic agents DNR and Ara-C. We therefore, incubated SIRT6 depleted cells with clinically relevant concentrations of either agents and assessed their viability. As showed in Fig.2D, significantly more cytotoxicity was observed in absence of SIRT6 compared with scramble control transfectants. Consistent with these data, the SIRT6 chemical inhibitor compound 1, (34, 35) was also found to sensitize cell lines as well as primary AML cells to DDAs. (Fig. 2 E-F) Together, these results are consistent with a leading role played by SIRT6 in regulating AML cells sensitivity to chemotherapy.

SIRT6 loss affects ATM/CHK2 pathway, as well as recruitment of repair factors to sites of DNA damage.

As SIRT6-depleted cells are more sensitive to genotoxic stress due to failure of DNA repair mechanisms, we next measured levels of proteins mediating DNA DSBs response after SIRT6 silencing. Although SIRT6 depletion did not affect the protein level of ATM, CHK2 or RPA, after DDAs treatment it markedly diminished their functional activity. Specifically, in scramble control, DDAs treatment induced RPA phosphorylation on Ser4 and Ser8, as well as increased ATM and CHK2 phosphorylation together with accumulation of lower-molecular-weight protein γH2AX. DDAs treatment did not induce the same effects (in term of phosphorylation of CHK2, RPA32, and ATM) in SIRT6-knockdown cells. Similarly, increase in γH2AX level was more pronounced in SIRT6-depleted OCI-AML2 and OCI-AML3 cells. (Fig.3A and Fig. S4) Overall, these observations identify a crucial role of SIRT6 in preserving genome integrity of AML cells through promotion of DNA repair mechanisms. Next, we asked whether SIRT6 also mediates the recruitment of DNA repair factors to

damage sites, which represents an attempt to preserve genomic integrity. We employed immunofluorescence to measure ability of AML cells expressing SIRT6 shRNA to recruit repair factors including 53BP1, Rad51, RPA and γH2AX, to the sites of DNA damage following DDAs treatment. As shown in Fig.3 B-D, genotoxic stress resulted in increased γH2AX foci formation as well as impaired Rad51, pRPA and 53BP1 foci formation in SIRT6-knockdown compared with SIRT6-wt AML cells. Therefore, the simultaneous presence of increased DNA damage and decreased DNA DSBs repair explains the observed hypersensitivity of these cells to DDAs.

SIRT6 maintains genome integrity by deacetylation of DNA-PKcs and CtIP in AML cells

To gain insights into specific function of SIRT6 in DNA damage context of AML cells, we characterized SIRT6-interacting proteins. (30, 36, 37) GFP-tagged SIRT6 was expressed in OCI-AML3 cells and then immunoprecipitated with anti-GFP antibody. Western blot analysis revealed that DNA-PKcs and CtIP were enriched in the GFP-SIRT6 immunoprecipitates (IPs), mainly after DDAs treatment. Importantly, SIRT6 inhibition by compound 1 heavily reduced levels of both proteins, also in the presence of genotoxic stress. (Fig.4A) Other SIRTs family proteins, such as SIRT1, did not associate with GFP-SIRT6 under these conditions, validating specificity of the assay. Analysis of endogenous SIRT6 IPs confirmed this association as well as its resistance to ethidium bromide, indicating that it is not due to DNA bridging (Fig.4B and Fig.S5) Our data therefore indicate that SIRT6 interacts physically with DNA-PKcs and CtIP in AML cells, and that this interaction increases rapidly upon genotoxic stress. Since SIRT6 is a histone deacetylase, we next tested whether acetylation status of interacting proteins was affected by SIRT6 depletion. Each endogenous protein was pulled down separately after treatment with DDAs in both SIRT6-wt and SIRT6-KD AML cells. Although we readily detected acetylation of DNA-PKcs as well as CtIP in SIRT6 wild-type cells, their acetylation was abrogated after DNR and Ara-C treatment. In contrast, DNA damage-induced deacetylation of these proteins was totally abolished in SIRT6 depleted cells. (Fig.4C and Fig. S6) These data suggest

that DNA-PKcs and CtIP are constitutively acetylated in AML cells, and are deacetylated by SIRT6 following genotoxic stimuli, thereby promoting DNA damage repair. This observation was further confirmed by treating AML cells overexpressing human SIRT6(H133Y) catalytic mutant with increased doses of DDAs. As shown in Fig.4D, DDAs treatment resulted in more pronounced anti-tumor effect in AML cells overexpressing the catalytically inactive mutant than wild type form of SIRT6, indicating that enzymatic activity is required for SIRT6 to maintain genome stability of AML cells.

Ongoing DNA damage is associated with intense replicative stress and high SIRT6 expression in AML cells.

Several studies have recently demonstrated a pervasive dysregulation of genomic stability in several cancers, including AML. (8, 38) To explore whether observed high SIRT6 expression was related to constitutive DNA damage and intense replicative stress observed in AML cells, we employed a chromosomal instability signature (CIN) (16) to categorize AML cell lines included in a published dataset (GSE59808). As shown in Fig.5A, a subset of approximately 40% AML cell lines demonstrated overexpression of probe sets belonging to CIN-signature. To confirm this finding, we next explored a panel of AML cell lines together with primary tumor cells. Six of 9 AML cell lines, as well as primary cells derived from ten AML patients, showed high γ-H2A.X staining (Fig. 5B-C) as well as activated DDR (Fig. 5D). Remarkably, this pattern was absent in normal PBMCs derived from healthy individuals, (Fig. 5C) as already reported. (39) Thus, such ongoing DNA damage observed in tumor cells did not induce an extensive cell death under basal conditions, suggesting existence of alternative mechanisms to escape apoptotic cell death triggered in normal cells.

We previously reported that SIRT6 preserves DNA integrity in MM cells.(15) To investigate whether such deacetylase affects instability also in AML cells, we categorized leukemia cell lines included in GSE59808 according to their SIRT6 expression levels. As shown in Fig.5E, AML cell lines with high

CIN-signature exhibited greater SIRT6 mRNA levels (p= 0.01). As a measure of specificity of this effect, we assessed gene expression profiles of AML cells based on their SIRT6 levels, using Gene Set Enrichment Analysis. (40) Remarkably, the gene expression profile defined by Carter et al. (16) significantly correlates with SIRT6 expression in AML cells (p = 0.02; Fig. 5F). In parallel, analysis on the entire set of transcription target gene signatures available from the Molecular Signatures Database (MSigDB) showed gene sets included in DNA replication and cell-cycle regulatory genes pathway as also significantly deregulated in these cells (data not shown), suggesting that SIRT6 drives DNA damage and activation of DNA damage response also in AML cells.

AML patients with SIRT6 overexpression show feature of genomic instability and poor prognosis

We next examined whether the broad DNA damage observed in AML patients-derived cells is also associated with SIRT6 mRNA levels. To this end, we probed samples from 5 data sets, including tumor and $CD34^+$ cells from healthy donors (GSE1159, GSE7186, GSE425, GSE12417 and GSE37642), for CIN gene expression signature. As shown in Fig. 6A this analysis sharply divided samples into two groups, with AML patients overexpressing probe sets belonging to CIN signature compared with cells derived from healthy individuals. To further characterize this data, we next interrogated a publically available data set of 524 cases of de novo AML, (41) observing that tumor samples can be split up into three groups, based on the expression of genes included in CIN signature: low, intermediate and high. (Fig. 6B) Importantly, this arrangement did not overlap with other features, including cytogenetic abnormalities and FLT3 mutations (data not shown). Next, we analyzed the prognostic significance of these findings observing that patients displaying higher CIN signature demonstrated poor prognosis compared with remaining patients. ($p<0.001$; Fig. 6C) Finally, we analyzed these AML patients using GSEA. As observed in AML cell lines, this analysis revealed that CIN signature was the most significantly altered pathway measured in patients classified on the basis of their SIRT6 expression level (p=0.03, FDR = 0.04; Fig. 6D); the DNA repair pathway and the BRCAness signature (42) also

differed in these patients subgroups. (Fig. S7 A,B) In line with these data, higher SIRT6 levels were observed in patients with high CIN signature than those with intermediate or low SIRT6 expression level. (Fig. 6E) Altogether our results suggest a link between SIRT6 and genomic instability also in AML patient-derived samples, justifying the highest SIRT6 levels observed in more aggressive disease subtypes.

SIRT6 inhibition makes AML blasts more sensitive to DNR treatment in NSG mice

To assess whether the biological results observed *in vitro* occurs also *in vivo*, we used two different xenotransplant mouse models of AML. First, U937 scramble or SIRT6-KD stably transduced cells were injected subcutaneously into NSG mice (n=20). After tumor engraftment, mice (n=5) of each group were randomly assigned to receive either 3 mg/kg of DNR administered intraperitoneally (at day 1 and 5) or vehicle control. (15) As in the *in vitro* setting, SIRT6 depletion made AML cells more sensitive to genotoxic agents, with a significant reduction of tumor growth in mice bearing these cells compared with tumors induced by AML cells carrying normal SIRT6 levels. Indeed, at 30^{th} day after tumor injection, mean tumor volume was 60 vs. 40 mm^2 , respectively (p=0.03; Fig.7A).

In a second *in-vivo* model, we intravenously injected human HL-60 cells, scramble or SIRT6 shRNA-transduced, into NSG mice (n□=20; □5 mice per condition). Once a systemic xenograft was confirmed (greater than 0.1% in peripheral blood of mice) the treatment regimen was initiated (1.5mg/kg of DNR administered intraperitoneally, for 3 days, or vehicle control). At 31^{st} day after cell transfer, flow cytometry evaluation of the circulating human CD45+ cells in the murine PB was performed to assess AML engraftment. As shown in Figure 7B, this analysis revealed a significant lower leukemia burden after DNR-treatment than vehicle, with SIRT6 depletion making these cells more sensitive to chemotherapy (the percentage of human engraftment: 0.9 ± 0.1% and 0.16 ± 0.01%, respectively, with p=0.006), as observed *in-vitro*. Tumor cells engraftment was measured also at 40^{th} day and results showed that SIRT6-depleted treated mice had significantly fewer tumor cells compared with relative

control. (Fig. 7C) Furthermore, as shown in Fig. 7D, Kaplan-Meier analyses indicated that DNR-treated mice injected with SIRT6-depleted survived significantly longer than those bearing tumors with normal SIRT6 levels (56 vs 39 days; p=0.004). Overall these data show that AML blasts depleted of SIRT6 are more sensitive to DDAs agents also in an *in-vivo* environment, suggesting therefore evaluation of SIRT6 inhibition as a novel strategy to enhance DDAs sensitivity in AML patients.

DISCUSSION

The efficiency of DNA-repair and DNA damage-response pathways, affects both cancer susceptibility and responses to genotoxic agent-based therapies. (33) As a result, synthetic lethal approaches to specifically kill cancer cells, that are dependent on compensatory DNA repair pathways, are emerging as vulnerability that can be therapeutically targeted. (39, 43-45) In this context, we have recently showed that the chromatin-bound factor, SIRT6, safeguards the genome of MM cells. (15) Here, we further extend these observations to AML cells and demonstrate that SIRT6 controls leukemogenesis and tumor growth by struggling with their instability. Indeed, we show that defects in SIRT6 expression or activity sensitize AML cells to genotoxic agents, leading to a significant blast-cell counts reduction, and to prolonged survival in AML mice models. Co-IP experiments have also demonstrated that SIRT6 deacetylates DNA-PKcs and CtIP, resulting in efficient DNA repair mechanisms and integrity of AML cells. In contrast, loss of SIRT6 enzymatic activity enhances instability which in turn sensitizes leukemia cells to DDAs. Overall our data suggest an innovative strategy to enhance efficacy of chemotherapy, which still remain the backbone for treatment, in AML. Additionally, based on low SIRT6 levels detected in normal $CD34^+$ hematopoietic progenitors, a favorable therapeutic index of such approach is also warranted.

Genomic instability is one of the distinctive markers of tumor cells providing them additional capabilities crucial for tumorigenesis. (46-50) In hematological cancers, the relevance of such feature, and the mechanisms underlying instability are largely unknown. (15, 30, 51-57) Based on our data, we assume that pervasive DNA damage observed in AML cells is reliant on genes such as SIRT6, that when disrupted, lead to further instability. (58, 59) The prominent role exerted by SIRT6 on leukemogenesis is reinforced by its prognostic relevance, as observed in primary AML samples. Indeed, SIRT6 overexpression is associated with greater instability and worse prognosis. As a result genetic inactivation of this chromatin remodeler, triggers growth advantage and DNA repair weakening

that in turn cause greater DDAs sensitivity. A comprehensive genomic analysis revealed that AML patients harbor several genetic alteration, (66) including FLT3-ITD which primes leukemic cells to genotoxic stress-induced. (12) Here we observed higher SIRT6 mRNA expression levels in AML patients carrying FLT3-ITD mutant, providing further evidence for a direct link between SIRT6 and genomic instability in AML. Nevertheless these effects were not related to other specific genetic makeup, suggesting that SIRT6 acts on genomic stability of AML regardless of its specific genomic landscape.

As cancer genome is itself reflective of phenotypic properties, specific gene signatures have been employed to predict clinical outcome and identify prognostically relevant feature in different cancer subtypes. (60, 61) Similarly, measurement of genomic instability degree, by leveraging specific genes signature, provides a valuable tool for prognostic stratification. (62) Based on our data, here we asked whether consequences of aberrant DNA repair are reflected in genomic features, and how these events are associated with SIRT6 expression levels in AML cells. Therefore, we analyzed published databases for abnormal expression of genes belonging to chromosomal instability signature (14), recently identified as instability biomarker. (43) As shown in Figure 6, the CIN-based stratification highly correlated with SIRT6 mRNA levels: greater instability was observed in patients harboring highest SIRT6 level which results in poor prognosis. Thus, our data pinpoint SIRT6 as a valuable feature to segregate AML patients into distinct molecular and biological classes.

Besides SIRT6, also SIRT1 promotes genomic integrity of tumor cells, proposing on overlapping function. (52, 63) In such a scenario, a broad gene expression analysis of SIRTs family members revealed SIRT6 and SIRT1 as top ranked, thus supporting the crucial role of these two proteins for AML cells. (Fig. S8 A-B) SIRT6 is a chromatin-bound deacetylase that participates to DNA double-strand break repair by affecting activity of several proteins, including CtIP, PARP1, DNA-PK complex and SNF2H at DNA damage sites. (30, 32, 36, 56) Here we show that AML cells, after genotoxic

stress, rapidly recruit SIRT6 to DNA damaged sites where it deacetylates and promotes activity of DNA-PKcs and CtIP. In contrast, compromising SIRT6 activity decreases repair mechanisms resulting in greater DDAs cytotoxicity both *in vitro* and in murine xenograft models of human AML.

In summary, among the potential mechanisms that could cause instability, the disruption of DNA repair complex is an intriguing avenue that anti-cancer therapies may pursue to increase activity of currently used therapeutics. While analysis of larger cohorts of patients may yet identify additional data on specific impact of SIRT6 on genomic instability, here we identify such deacetylase as vulnerability to be exploited in developing future intervention strategies, speculating also its role as surrogate genetic marker for instability in AML patients. Overall, our study provides proof-of-concept that depletion of SIRT6 represents a novel strategy to selectively target AML cells enhancing their sensitivity to currently used chemotherapies.

REFERENCES

1. Sant M, Allemani C, Tereanu C, et al. Incidence of hematologic malignancies in Europe by morphologic subtype: results of the HAEMACARE project. Blood. 2010;116(19):3724-3734.

2. Ferrara F, Schiffer CA. Acute myeloid leukaemia in adults. Lancet. 2013;381(9865):484-495.

3. Dombret H, Gardin C. An update of current treatments for adult acute myeloid leukemia. Blood. 2016;127(1):53-61.

4. De Kouchkovsky I, Abdul-Hay M. Acute myeloid leukemia: a comprehensive review and 2016 update. Blood Cancer J. 2016;6(7):e441.

5. Guolo F, Minetto P, Clavio M, et al. High feasibility and antileukemic efficacy of fludarabine, cytarabine, and idarubicin (FLAI) induction followed by risk-oriented consolidation: A critical review of a 10-year, single-center experience in younger, non M3 AML patients. Am J Hematol. 2016;91(8):755-762.

6. Burnett AK, Hills RK, Milligan DW, et al. Attempts to optimize induction and consolidation treatment in acute myeloid leukemia: results of the MRC AML12 trial. J Clin Oncol. 2010;28(4):586-595.

7. Lowenberg B, Rowe JM. Introduction to the review series on advances in acute myeloid leukemia (AML). Blood. 2016;127(1):1.

8. Esposito MT, So CW. DNA damage accumulation and repair defects in acute myeloid leukemia: implications for pathogenesis, disease progression, and chemotherapy resistance. Chromosoma. 2014;123(6):545-561.

9. Liu H, Takeda S, Kumar R, et al. Phosphorylation of MLL by ATR is required for execution of mammalian S-phase checkpoint. Nature. 2010;467(7313):343-346.

10. Morgado-Palacin I, Day A, Murga M, et al. Targeting the kinase activities of ATR and ATM exhibits antitumoral activity in mouse models of MLL-rearranged AML. Sci Signal. 2016;9(445):ra91.

11. Fan J, Li L, Small D, Rassool F. Cells expressing FLT3/ITD mutations exhibit elevated repair errors generated through alternative NHEJ pathways: implications for genomic instability and therapy. Blood. 2010;116(24):5298-5305.

12. Sallmyr A, Fan J, Datta K, et al. Internal tandem duplication of FLT3 (FLT3/ITD) induces increased ROS production, DNA damage, and misrepair: implications for poor prognosis in AML. Blood. 2008;111(6):3173-3182.

13. Kugel S, Mostoslavsky R. Chromatin and beyond: the multitasking roles for SIRT6. Trends Biochem Sci. 2014;39(2):72-81.

14. Finkel T, Deng CX, Mostoslavsky R. Recent progress in the biology and physiology of sirtuins. Nature. 2009;460(7255):587-591.

15. Cea M, Cagnetta A, Adamia S, et al. Evidence for a role of the histone deacetylase SIRT6 in DNA damage response of multiple myeloma cells. Blood. 2016;127(9):1138-1150.

16. Carter SL, Eklund AC, Kohane IS, Harris LN, Szallasi Z. A signature of chromosomal instability inferred from gene expression profiles predicts clinical outcome in multiple human cancers. Nat Genet. 2006;38(9):1043-1048.

17. Salvestrini V, Orecchioni S, Talarico G, et al. Extracellular ATP induces apoptosis through P2X7R activation in acute myeloid leukemia cells but not in normal hematopoietic stem cells. Oncotarget. 2017;8(4):5895-5908.

18. Bae JS, Park SH, Jamiyandorj U, et al. CK2alpha/CSNK2A1 Phosphorylates SIRT6 and Is Involved in the Progression of Breast Carcinoma and Predicts Shorter Survival of Diagnosed Patients. Am J Pathol. 2016;186(12):3297-3315.

19. Ran LK, Chen Y, Zhang ZZ, et al. SIRT6 Overexpression Potentiates Apoptosis Evasion in Hepatocellular Carcinoma via BCL2-Associated X Protein-Dependent Apoptotic Pathway. Clin Cancer Res. 2016;22(13):3372-3382.

20. Azuma Y, Yokobori T, Mogi A, et al. SIRT6 expression is associated with poor prognosis and chemosensitivity in patients with non-small cell lung cancer. J Surg Oncol. 2015;112(2):231-237.

21. Ming M, Han W, Zhao B, et al. SIRT6 promotes COX-2 expression and acts as an oncogene in skin cancer. Cancer Res. 2014;74(20):5925-5933.

22. Mostoslavsky R, Chua KF, Lombard DB, et al. Genomic instability and aging-like phenotype in the absence of mammalian SIRT6. Cell. 2006;124(2):315-329.

23. Michishita E, Park JY, Burneskis JM, Barrett JC, Horikawa I. Evolutionarily conserved and nonconserved cellular localizations and functions of human SIRT proteins. Mol Biol Cell. 2005;16(10):4623-4635.

24. Liszt G, Ford E, Kurtev M, Guarente L. Mouse Sir2 homolog SIRT6 is a nuclear ADP-ribosyltransferase. J Biol Chem. 2005;280(22):21313-21320.

25. Stirewalt DL, Meshinchi S, Kopecky KJ, et al. Identification of genes with abnormal expression changes in acute myeloid leukemia. Genes Chromosomes Cancer. 2008;47(1):8-20.

26. Eppert K, Takenaka K, Lechman ER, et al. Stem cell gene expression programs influence clinical outcome in human leukemia. Nat Med. 2011;17(9):1086-1093.

27. Bullinger L, Dohner K, Bair E, et al. Use of gene-expression profiling to identify prognostic subclasses in adult acute myeloid leukemia. N Engl J Med. 2004;350(16):1605-1616.

28. Liu Y, Xie QR, Wang B, et al. Inhibition of SIRT6 in prostate cancer reduces cell viability and increases sensitivity to chemotherapeutics. Protein Cell. 2013;4(9):702-710.

29. Huen MS, Chen J. The DNA damage response pathways: at the crossroad of protein modifications. Cell Res. 2008;18(1):8-16.

30. Kaidi A, Weinert BT, Choudhary C, Jackson SP. Human SIRT6 promotes DNA end resection through CtIP deacetylation. Science. 2010;329(5997):1348-1353.

31. Van Meter M, Mao Z, Gorbunova V, Seluanov A. Repairing split ends: SIRT6, mono-ADP ribosylation and DNA repair. Aging. 2011;3(9):829-835.

32. Toiber D, Erdel F, Bouazoune K, et al. SIRT6 recruits SNF2H to DNA break sites, preventing genomic instability through chromatin remodeling. Mol Cell. 2013;51(4):454-468.

33. Curtin NJ. DNA repair dysregulation from cancer driver to therapeutic target. Nat Rev Cancer. 2012;12(12):801-817.

34. Sociali G, Galeno L, Parenti MD, et al. Quinazolinedione SIRT6 inhibitors sensitize cancer cells to chemotherapeutics. Eur J Med Chem. 2015;102:530-539.

35. Sociali G, Magnone M, Ravera S, et al. Pharmacological Sirt6 inhibition improves glucose tolerance in a type 2 diabetes mouse model. FASEB J. 2017;31(7):3138-3149.

36. McCord RA, Michishita E, Hong T, et al. SIRT6 stabilizes DNA-dependent protein kinase at chromatin for DNA double-strand break repair. Aging. 2009;1(1):109-121.

37. Simeoni F, Tasselli L, Tanaka S, et al. Proteomic analysis of the SIRT6 interactome: novel links to genome maintenance and cellular stress signaling. Sci Rep. 2013;3:3085.

38. Rebechi MT, Pratz KW. Genomic instability is a principle pathologic feature of FLT3 ITD kinase activity in acute myeloid leukemia leading to clonal evolution and disease progression. Leuk Lymphoma. 2017:1-11.

39. Cottini F, Hideshima T, Xu C, et al. Rescue of Hippo coactivator YAP1 triggers DNA damage-induced apoptosis in hematological cancers. Nat Med. 2014;20(6):599-606.

40. Subramanian A, Tamayo P, Mootha VK, et al. Gene set enrichment analysis: a knowledge-based approach for interpreting genome-wide expression profiles. Proc Natl Acad Sci U S A. 2005;102(43):15545-15550.

41. Taskesen E, Bullinger L, Corbacioglu A, et al. Prognostic impact, concurrent genetic mutations, and gene expression features of AML with CEBPA mutations in a cohort of 1182 cytogenetically

normal AML patients: further evidence for CEBPA double mutant AML as a distinctive disease entity. Blood. 2011;117(8):2469-2475.

42. Konstantinopoulos PA, Spentzos D, Karlan BY, et al. Gene expression profile of BRCAness that correlates with responsiveness to chemotherapy and with outcome in patients with epithelial ovarian cancer. J Clin Oncol. 2010;28(22):3555-3561.

43. Cottini F, Hideshima T, Suzuki R, et al. Synthetic Lethal Approaches Exploiting DNA Damage in Aggressive Myeloma. Cancer Discov. 2015;5(9):972-987.

44. Ka NL, Na TY, Na H, et al. NR1D1 recruitment to sites of DNA damage inhibits repair and is associated with chemosensitivity of breast cancer. Cancer Res. 2017;77(9):2453-2463.

45. Brown JS, O'Carrigan B, Jackson SP, Yap TA. Targeting DNA Repair in Cancer: Beyond PARP Inhibitors. Cancer Disc. 2017;7(1):20-37.

46. Hanahan D, Weinberg RA. Hallmarks of cancer: the next generation. Cell. 2011;144(5):646-674.

47. Friedberg EC. DNA damage and repair. Nature. 2003;421(6921):436-440.

48. Abraham RT. Checkpoint signaling: epigenetic events sound the DNA strand-breaks alarm to the ATM protein kinase. BioEssays. 2003;25(7):627-630.

49. Jackson SP, Bartek J. The DNA-damage response in human biology and disease. Nature. 2009;461(7267):1071-1078.

50. Stratton MR, Campbell PJ, Futreal PA. The cancer genome. Nature. 2009;458(7239):719-724.

51. Kim HS, Vassilopoulos A, Wang RH, et al. SIRT2 maintains genome integrity and suppresses tumorigenesis through regulating APC/C activity. Cancer Cell. 2011;20(4):487-499.

52. Wang RH, Sengupta K, Li C, et al. Impaired DNA damage response, genome instability, and tumorigenesis in SIRT1 mutant mice. Cancer Cell. 2008;14(4):312-323.

53. Jeong SM, Xiao C, Finley LW, et al. SIRT4 has tumor-suppressive activity and regulates the cellular metabolic response to DNA damage by inhibiting mitochondrial glutamine metabolism. Cancer Cell. 2013;23(4):450-463.

54. Marquardt JU, Fischer K, Baus K, et al. Sirtuin-6-dependent genetic and epigenetic alterations are associated with poor clinical outcome in hepatocellular carcinoma patients. Hepatology. 2013;58(3):1054-1064.

55. Michishita E, McCord RA, Berber E, et al. SIRT6 is a histone H3 lysine 9 deacetylase that modulates telomeric chromatin. Nature. 2008;452(7186):492-496.

56. Mao Z, Hine C, Tian X, et al. SIRT6 promotes DNA repair under stress by activating PARP1. Science. 2011;332(6036):1443-1446.

57. Mao Z, Tian X, Van Meter M, Ke Z, Gorbunova V, Seluanov A. Sirtuin 6 (SIRT6) rescues the decline of homologous recombination repair during replicative senescence. Proc Natl Acad Sci U S A. 2012;109(29):11800-11805.

58. Sperlazza J, Rahmani M, Beckta J, et al. Depletion of the chromatin remodeler CHD4 sensitizes AML blasts to genotoxic agents and reduces tumor formation. Blood. 2015;126(12):1462-1472.

59. Cea M, Soncini D, Fruscione F, et al. Synergistic interactions between HDAC and sirtuin inhibitors in human leukemia cells. PloS One. 2011;6(7):e22739.

60. Stratton MR. Exploring the genomes of cancer cells: progress and promise. Science. 2011;331(6024):1553-1558.

61. Negrini S, Gorgoulis VG, Halazonetis TD. Genomic instability--an evolving hallmark of cancer. Nature reviews Mol Cell Biol. 2010;11(3):220-228.

62. Chin L, Gray JW. Translating insights from the cancer genome into clinical practice. Nature. 2008;452(7187):553-563.

63. Sasca D, Hahnel PS, Szybinski J, et al. SIRT1 prevents genotoxic stress-induced p53 activation in acute myeloid leukemia. Blood. 2014;124(1):121-133.

FIGURES LEGENDS

Figure 1. SIRT6 is highly enriched in AML and its expression confers poor prognosis. (A) Protein lysates from a panel of AML cell lines (*left panel*), primary patient-derived AML cultures or normal PBMCs (*right panel*) were analyzed for SIRT6 expression by western blot. GAPDH was used as loading control. The quantification of SIRT6/GAPDH ratios is showed below. One experiment of two is shown. **(B)** Six AML cell lines were analyzed for SIRT6 (green) by immunofluorescence. 4′,6-diamidino-2-phenylindole nuclear stain is shown in blue. **Original magnification ×20. (C)** Box plot distributions of SIRT6 gene expression levels in normal hematopoietic cells from healthy donors and leukemic $CD34^+$ blasts from AML patients (N=300), combining data from GSE1159, GSE9476 and GSE30377 (using the probe set 219613_s_at). Normal hematopoietic samples included $CD34^+$ selected cells (N= 18; 8 from BM and 10 from PB), $CD34^+$ $CD38^-$ cells (N= 10), unselected bone marrows (N= 10), and unselected peripheral bloods (N= 6). The numbers below graph are the samples per group (N=). ns, not significant, **P < 0.05, ***P < 0.001 (one-way analysis of variance (ANOVA) with expression data log(2) transformed). **(D)** Increased SIRT6 mRNA expression is observed in AML patients ($CD34^+$ blast cells) relative to normal controls ($CD34^+$ cells collected from peripheral blood or bone marrow of healthy donors; unpaired *t* test; **p=0.006;*p=0.02). GAPDH mRNA expression was used as an internal control. (**E**) Survival curves relative to SIRT6 expression in 100 individuals affected by AML diagnosed at our clinic. The patient group with higher SIRT6 expression (red line) had shorter overall survival than the patient cohort with lower SIRT6 expression (blue line) (log-rank test). The SIRT6 mRNA median value was use to split AML patients.

Figure 2. SIRT6 affects proliferation and vulnerability to DNA-Damage Agents in AML cells. (A) SIRT6 silencing in THP-1 and U937 cells using a lentiviral delivery system. On the left, western blot analysis in pGIPz-infected cells after 48 h of selection with 1 μg ml-1 puromycin. In the center, cell numbers evaluated by cell counting with trypan blue exclusion. On the right AML-engineered cells

were assessed for cell number and **(B)** cell-cycle progression. All data throughout the panel are shown as the mean values ± s.d. of triplicates. ns: not significant, *P < 0.01, **P < 0.001 (Student's t test) **(C)** Representative western blots showing DDR pathway deregulation in THP-1 cells depleted of SIRT6 compared with control. GAPDH was used as loading control. One representative blot of two is shown. **(D)** OCI-AML-2 and OCI-AML-3 cells were transduced with a scrambled shRNA (CTR) or with an anti-SIRT6 shRNA (#911). Cells were used for immunoblotting detection of SIRT6 or γ-tubulin expression (*upper insets*) or in viability experiments. For the latter 2 x 10^4 cells/well were plated in 96-well plates and incubated for 48h with or without DNR or ARA-C at the indicated concentration. Thereafter, dead cells were detected by propidium iodide staining and flow cytometry. 2 x 10^4 OCI-AML2 **(E)** and primary AML **(F)** cells/well were plated in 96-well plates and incubated for 72h w/ or w/o DNR/ARA-C (at the indicated concentration) w/ or w/o compound 1 from [34]. Thereafter, dead cells were detected by propidium iodide staining and flow cytometry. *0.04<p<0.01; **0.009<p<0.001; ***<0.0001.

Figure 3. SIRT6 affects ATM/CHK2 pathway, as well as recruitment of repair factors to sites of DNA damage in AML cells. (A) Indicated AML cells were engineered to express an anti-SIRT6 shRNA (#911). Next, cells were incubated 3 hours with or without DNR (0.1 uM), or Ara-C (1 uM). Subsequently, total and phosphorylated ATM, Chk2, and RPA as well as γH2AX levels were detected by immunoblotting. Detection of Rad51 and γH2AX **(B)**, pRPA **(C)**, 53BP1 **(D),** and DAPI was measured by confocal microscopy in OCI-AML2 cells expressing shRNA (clone #911) targeting SIRT6 or control and cultured with or without treatment with Ara-C (1μM) or DNR (0.1μM) for 1 h (Magnification: 40X). Each panel includes representative foci-containing cells graph, over three experiments. *0.04<p<0.01; **0.009<p<0.001

Figure 4. SIRT6 depletion/inhibition sensitizes AML cells to genotoxic agents by disrupting DNA repair machinery. (A) OCI-AML2 cells were engineered to express a GFP-tagged SIRT6. Cells were

stimulated with compound 1, DNR (0.1 uM), or Ara-C (1 uM) for three hours. Thereafter, cells were used for protein lysate generation. SIRT6 in the different samples was co-immunoprecipitated using an anti-GFP antibody. Finally, GFP, CtIP, DNA-PKcs and SIRT1 levels were detected by immunoblotting. **(B)** OCI-AML2 cells were stimulated with compound 1, w/ or w/o DNR (0.1 uM) for three hours. Thereafter, cells were used for protein lysate generation. Endogenous SIRT6 in the different samples was immunoprecipitated using an anti-SIRT6 antibody and CtIP, DNA-PKcs, SIRT6, and SIRT1 levels were detected by immunoblotting. **(C)** OCI-AML2 engineered to express an shRNAs targeting SIRT6 (#911) were stimulated w/ or w/o DNR (0.1 uM), or Ara-C (1 uM) for three hours. CtIP (upper) and DNA-PKcs (lower) were immunoprecipitated and CtIP, DNA-PKcs, acetylated proteins (pan-acetyl-antibody) and γ-tubulin were detected by immunoblotting. **(D)** Viability assays after Ara-C (*left*) or DNR (*right*) treatment of OCI-AML2 non transfected cells, as well as in OCI-AML2 cells overexpressing SIRT6 wild type or mutant (H133Y).*p=0.02; **p<0.001

Figure 5. Ongoing DNA damage and high CIN signature are associated with intense replicative stress and SIRT6 overexpression in AML cells. (A) Expression levels in a panel of 32 human AML cell lines for the probe sets corresponding to the chromosomal instability signature described in (16), using GSE59808. Red color for a gene indicates expression above the median and blue color indicates expression below the media. **(B)** Immunofluorescence staining of γ-H2A.X in AML cell lines and primary tumor cells; magnification: 40X. **(C)** Western blot analysis (one representative blot out of three) of γ-H2A.X in AML cell lines (top), AML patients' cells and PBMCs from healthy donors (down). GAPDH, glyceraldehyde 3-phosphate dehydrogenase. **(D)** 53BP1 and RAD51 number of foci in a panel of AML cells presenting with high DNA damage (red bracket) and low DNA damage (blue bracket). **(E)** SIRT6 expression was compared to CIN signature among AML cell lines in the GSE59808 data set. *p=0.04. **(F)** GSEA enrichment profile for AML cell lines (included in GSE59808) divided in high and low SIRT6 expression groups of chromosomal instability signature as annotated in

(16). The analysis pointed to an association between high SIRT6 levels and CIN in AML cells.

Figure 6. High CIN gene expression signature confers poor prognosis in AML and correlates with SIRT6 expression. (A) Heat map showing CIN signature in 1157 AML patients compared to $CD34^+$ cells derived from healthy individuals (GSE1159, GSE7186, GSE425, GSE12417 and GSE37642). Red color for a gene indicates expression above the median and blue color indicates expression below the media. **(B)** Expression levels for the probe sets corresponding to the chromosomal instability signature using GEP data of 524 AML patients (GSE14468). **(C)** Kaplan-Meyer survival curves of AML patients showed in panel B based on their CIN gene expression signature. **(D)** GSEA enrichment profiles for AML patients included in GSE14468, divided in high and low SIRT6 expression groups of CIN signature as described in (16). The analysis pointed to an association between high SIRT6 levels and CIN in AML cells. **(E)** SIRT6 expression was compared to CIN signature in AML patients described in GSE14468 data set. **p=0.001; ***p=0.0001

Figure 7. SIRT6 inhibition makes AML blasts more sensitive to DNR treatment in NSG mice. (A) Growth of U937 control and SIRT6-depleted xenografts in mice treated with vehicle or DNR (3mg/kg i.p. day 1 and +4) at 20^{th} day after tumor engraftment. *p=0.036. Data are mean tumor volume ± SD. **(B)** 1×10^6 of scramble or shSIRT6-expressing HL-60 cells were engrafted into NSG mice (n= 20) by tail-vein injection. Once a systemic xenograft was confirmed, mice were randomized to receive DNR (1.5 mg/kg for 3 days) (treated group) or vehicle (control group). The histogram represents percentage of human $CD45^+$ cells in mice, at 31^{st} day post engraftment. Data are represented as mean ± SEM. *p = 0.006. **(C)** Representative flow cytometric dot plots representing tumor engraftment evaluated at 40^{th} day post-injection. **(D)** Kaplan-Meier survival plot showing median survival of mice injected with tumors w/wo SIRT6 before and after treatment with vehicle or DNR.

Figure 1

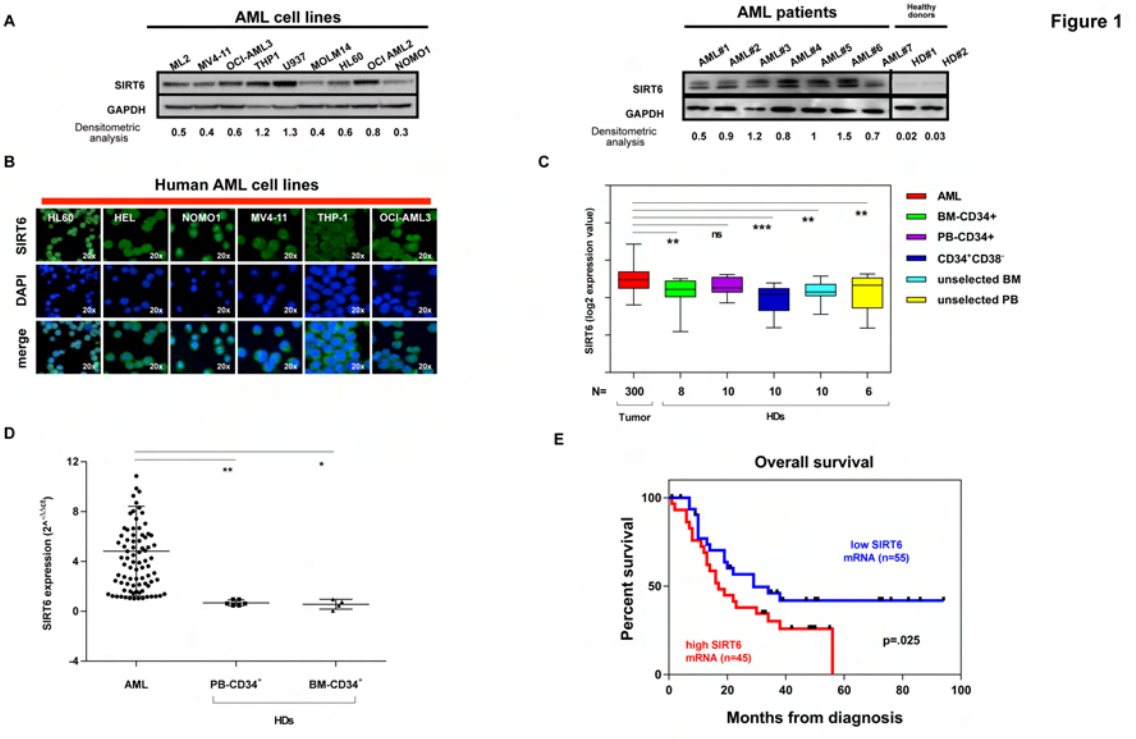
A
AML cell lines
ML2
MV4-11
OCI-AML3
THP1
U937
MOLM14
HL60
OCI AML2
NOMO1
SIRT6
GAPDH
Densitometric analysis
0.5 0.4 0.6 1.2 1.3 0.4 0.6 0.8 0.3
AML patients
Healthy donors
AML#1
AML#2
AML#3
AML#4
AML#5
AML#6
AML#7
HD#1
HD#2
SIRT6
GAPDH
Densitometric analysis
0.5 0.9 1.2 0.8 1 1.5 0.7 0.02 0.03
B
Human AML cell lines
HL60
HEL
NOMO1
MV4-11
THP-1
OCI-AML3
SIRT6
DAPI
merge
20x
C
SIRT6 (log2 expression value)
**
ns
***
**
**
AML
BM-CD34+
PB-CD34+
CD34+CD38-
unselected BM
unselected PB
N= 300 8 10 10 10 6
Tumor
HDs
D
SIRT6 expression (2^-ΔΔCt)
**
*
AML
PB-CD34+
BM-CD34+
HDs
E
Overall survival
Percent survival
low SIRT6 mRNA (n=55)
high SIRT6 mRNA (n=45)
p=.025
Months from diagnosis

Figure 2

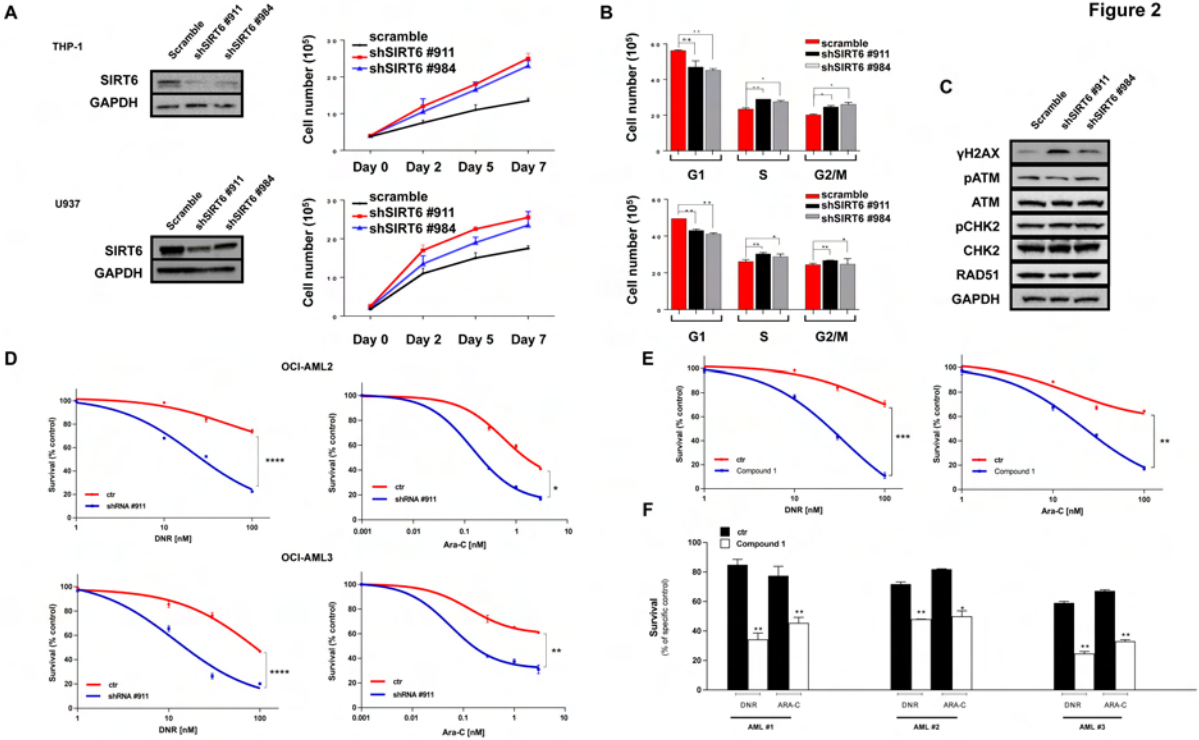
A
THP-1
Scramble
shSIRT6 #911
shSIRT6 #984
SIRT6
GAPDH
scramble
shSIRT6 #911
shSIRT6 #984
Cell number (10^5)
Day 0
Day 2
Day 5
Day 7
U937
B
G1
S
G2/M
C
γH2AX
pATM
ATM
pCHK2
CHK2
RAD51
GAPDH
D
OCI-AML2
OCI-AML3
Survival (% control)
ctr
shRNA #911
DNR [nM]
Ara-C [nM]
E
Compound 1
F
Survival
(% of specific control)
AML #1
AML #2
AML #3

Figure 3

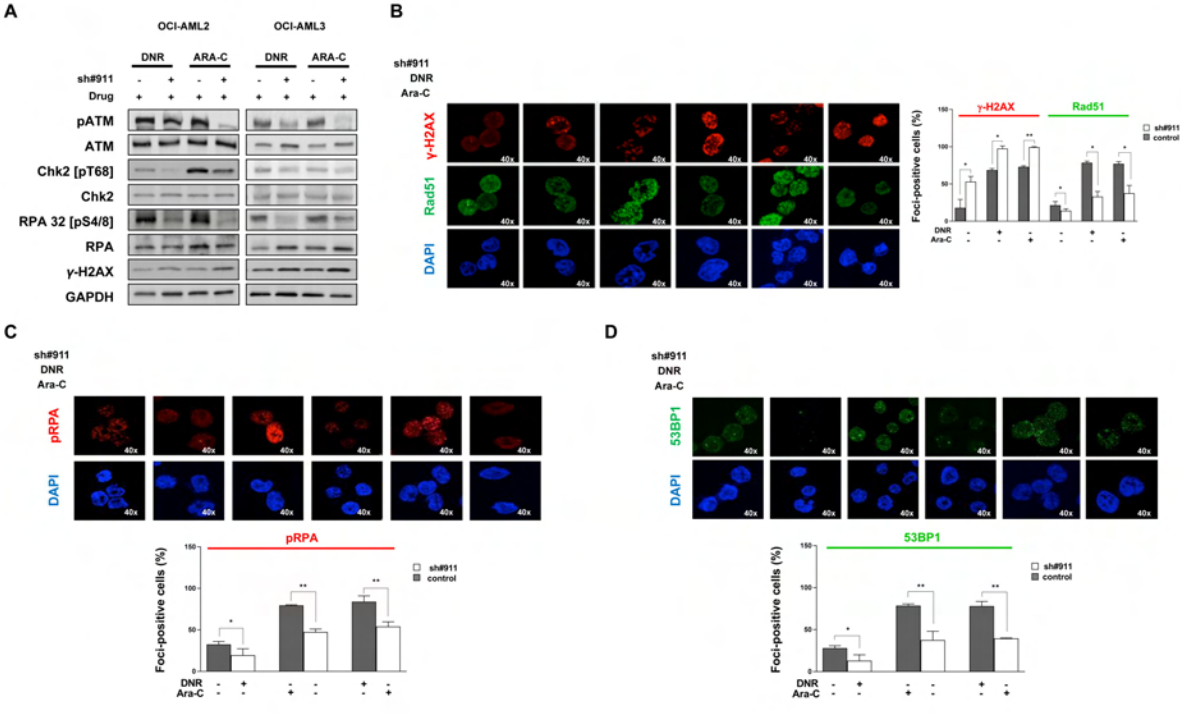
A
OCI-AML2
OCI-AML3
DNR
ARA-C
DNR
ARA-C
sh#911
Drug
pATM
ATM
Chk2 [pT68]
Chk2
RPA 32 [pS4/8]
RPA
γ-H2AX
GAPDH
B
sh#911
DNR
Ara-C
γ-H2AX
Rad51
DAPI
40x
γ-H2AX
Rad51
Foci-positive cells (%)
sh#911
control
DNR
Ara-C
C
sh#911
DNR
Ara-C
pRPA
DAPI
40x
pRPA
Foci-positive cells (%)
sh#911
control
DNR
Ara-C
D
sh#911
DNR
Ara-C
53BP1
DAPI
40x
53BP1
Foci-positive cells (%)
sh#911
control
DNR
Ara-C

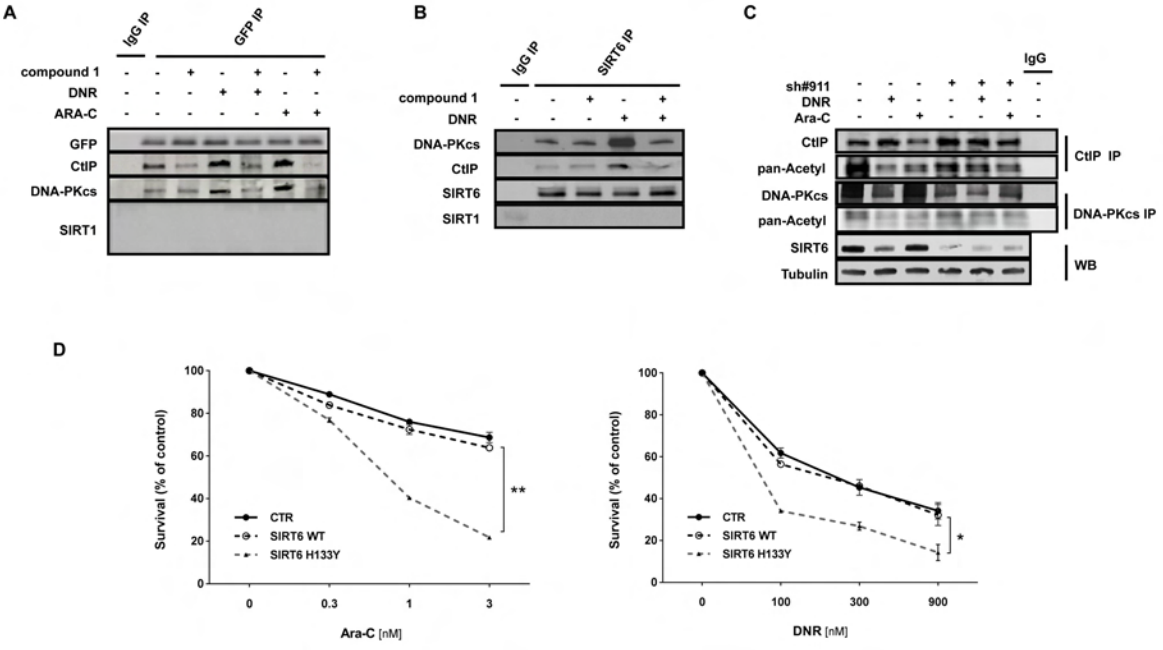
A
IgG IP
GFP IP
compound 1
DNR
ARA-C
GFP
CtIP
DNA-PKcs
SIRT1
B
IgG IP
SIRT6 IP
compound 1
DNR
DNA-PKcs
CtIP
SIRT6
SIRT1
C
IgG
sh#911
DNR
Ara-C
CtIP
pan-Acetyl
DNA-PKcs
pan-Acetyl
SIRT6
Tubulin
CtIP IP
DNA-PKcs IP
WB
D
Survival (% of control)
CTR
SIRT6 WT
SIRT6 H133Y
**
Ara-C [nM]
0
0.3
1
3
Survival (% of control)
CTR
SIRT6 WT
SIRT6 H133Y
*
DNR [nM]
0
100
300
900

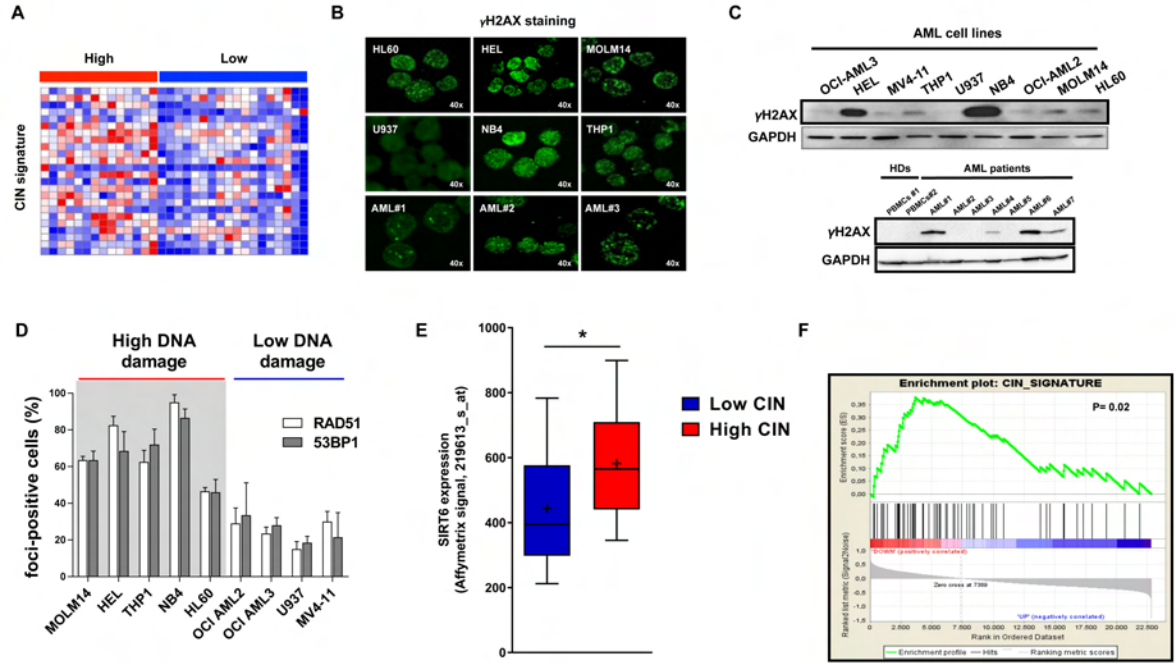
A
High
Low
CIN signature
B
γH2AX staining
HL60
HEL
MOLM14
U937
NB4
THP1
AML#1
AML#2
AML#3
40x
C
AML cell lines
OCI-AML3
HEL
MV4-11
THP1
U937
NB4
OCI-AML2
MOLM14
HL60
γH2AX
GAPDH
HDs
AML patients
PBMCs #1
PBMCs#2
AML#1
AML#2
AML#3
AML#4
AML#5
AML#6
AML#7
γH2AX
GAPDH
D
High DNA damage
Low DNA damage
foci-positive cells (%)
RAD51
53BP1
MOLM14
HEL
THP1
NB4
HL60
OCI AML2
OCI AML3
U937
MV4-11
E
SIRT6 expression (Affymetrix signal, 219613_s_at)
*
Low CIN
High CIN
F
Enrichment plot: CIN_SIGNATURE
P= 0.02
Enrichment score (ES)
'DOWN' (positively correlated)
Zero cross at 7389
'UP' (negatively correlated)
Ranked list metric (Signal2Noise)
Rank in Ordered Dataset
Enrichment profile
Hits
Ranking metric scores

Figure 6

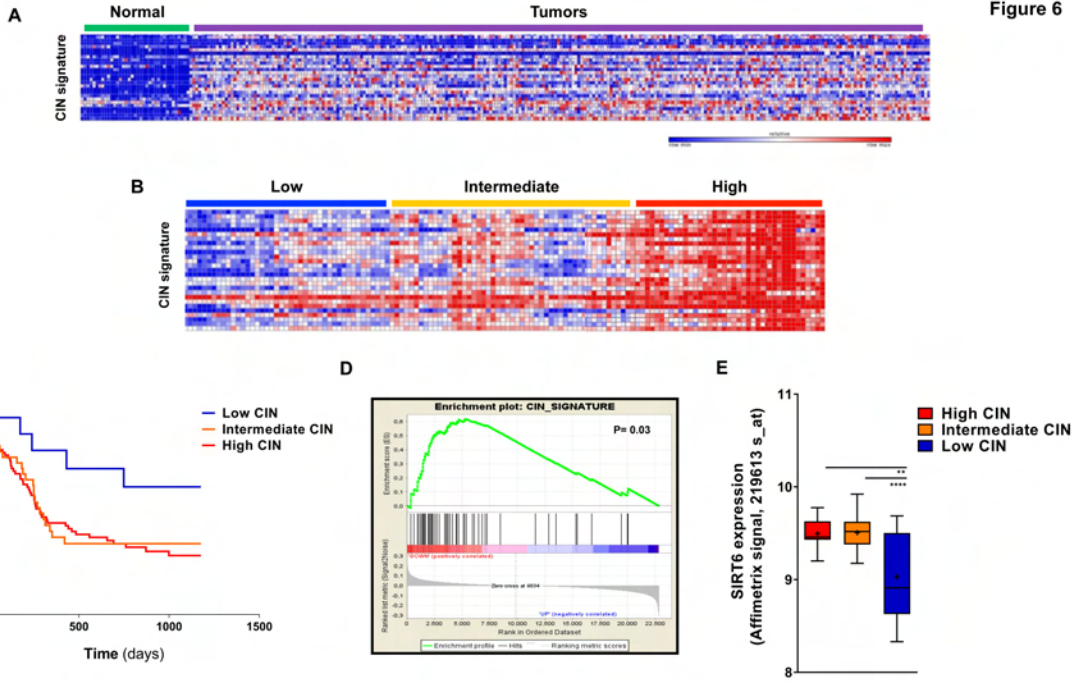
A
Normal
Tumors
CIN signature
B
Low
Intermediate
High
CIN signature
C
Low CIN
Intermediate CIN
High CIN
Survival (%)
Time (days)
D
Enrichment plot: CIN_SIGNATURE
P= 0.03
Rank in Ordered Dataset
Enrichment profile
Hits
Ranking metric scores
E
High CIN
Intermediate CIN
Low CIN
SIRT6 expression
(Affimetrix signal, 219613 s_at)

Figure 7

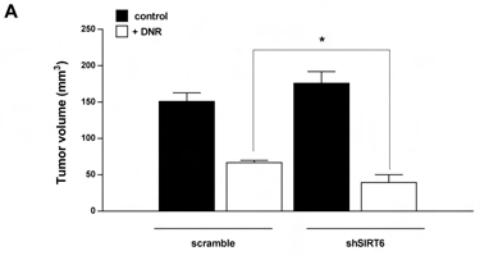
A
control
+ DNR
Tumor volume (mm3)
250
200
150
100
50
0
*
scramble
shSIRT6

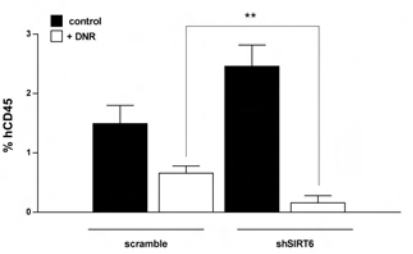
B
control
+ DNR
% hCD45
3
2
1
0
**
scramble
shSIRT6

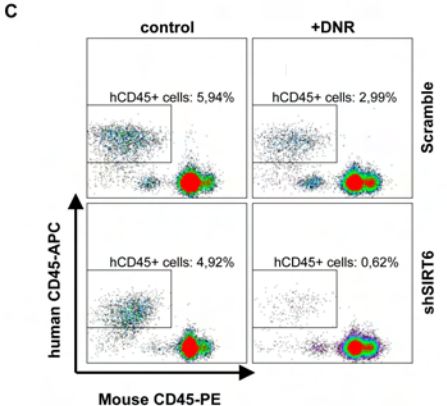
C
control
+DNR
hCD45+ cells: 5,94%
hCD45+ cells: 2,99%
Scramble
hCD45+ cells: 4,92%
hCD45+ cells: 0,62%
shSIRT6
human CD45-APC
Mouse CD45-PE

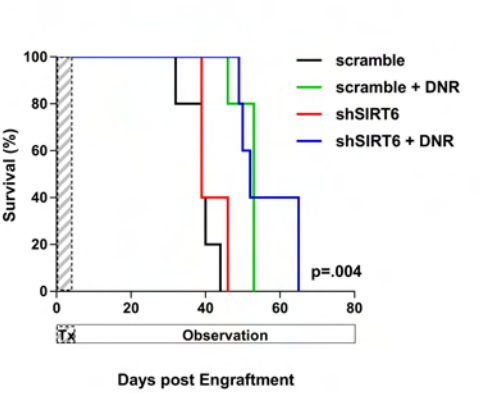
D
Survival (%)
100
80
60
40
20
0
scramble
scramble + DNR
shSIRT6
shSIRT6 + DNR
p=.004
0
20
40
60
80
TX
Observation
Days post Engraftment

SUPPLEMENTAL EXPERIMENTAL PROCEDURES

Gene editing by lentiviral transgenesis

SIRT6 was knocked-down using a pGIPz vector (Thermo Scientific, Pittsburg, PA) containing the target sequence (clone#984: TGCATTGAGGACTTTTCCA; clone#911: ACAAGTAACAAAGTGAGAC) or scramble control, according to manufacturer's specifications. To obtain stable silenced cells, the following protocol was used. 293T cells were plated (300,000 cells on 6-cm plates) in DMEM, 5% FBS, and 0.1% penicillin-streptomycin. After 24 h when cells were 60–70% confluent, 6,000 ng of the vector of interest together with Trans-Lentiviral Packaging Mix were co-transfected with CaCl2 (Thermo Scientific, Pittsburg, PA). After 12 h, the 293T medium was changed with DMEM, 20% FBS, and 10% penicillin-streptomycin to promote viral production. 24 and 48 h after transfection, the supernatant containing lentiviral particles was harvested, filtered with a 0.45-μm-diameter filter, and used to infect 2,500,000 AML cells. AML cells were spinoculated at 750g for 45 min with 8 μg ml−1 polybrene, (Santa Cruz Biotechnologies, CA) incubated with viral supernatant for 6 h and left in culturing medium. After the second cycle of infection, cells were selected with a suitable concentration of puromycin (2 μg ml−1). 48 and 72 h after selection, the transduction efficiency was approximated by counting the proportion of cells expressing the fluorescent protein (GFP) using a fluorescence microscope (Nikon Eclipse 80i, Nikin, Melville, NY); and the knockdown efficiency was validated by detecting SIRT6 protein level by WB analysis.(1) Further experiments were performed on SIRT6-depleted AML cells generated with sh#911 infection, which represented the most efficient approach.

Gene Expression Analysis

Gene expression profiling data were derived from publicly available Gene Expression Omnibus (GEO) datasets profiled on Affymetrix GeneChip Human Genome U133A or Plus 2.0 arrays, available at

accession numbers GSE59808, GSE1159, GSE7186, GSE425, GSE12417 GSE37642, GSE30377, GSE9476 and GSE14468. GSE1159, GSE39377 and GSE9476 samples' datasets were normalized together by Robust Multi-array Average procedure (2) and then re-annotated using Chip Definition Files from BrainArray libraries version 20.0.0. (3) ComBat function of sva package (available at http://www.bioconductor.org) was used to remove batch effects. (4) The Affymetrix U133 Plus 2.0 GEPs were derived from publicly available Gene Expression Omnibus (GEO) datasets accession numbers GSE59808, GSE1159, GSE7186, GSE425, GSE12417 GSE37642, GSE30377, GSE9476 and GSE14468). GSEA was performed as previously described (5) (GSEAv2.0 at http://www.broad.mit.edu/gsea) using gene set as permutation type and 1,000 permutations and signal to noise as metric for ranking genes. Both absolute and real data preprocessing were performed with GenePattern (http://genepattern.broadinstitute.org/gp/pages/login.jsf).

In vivo studies

Experiments were carried out on non-obese diabetic severe combined immunodeficient (NOD/SCID) interleukin-2 receptor g (IL-2Rg)–null (NSG) mice, 6 to 8-weeks-old. NSG mice were bred and housed under pathogen-free conditions in the animal facilities at the European Institute of Oncology–Italian Foundation for Cancer Research Institute of Molecular Oncology (IEO-IFOM, Milan, Italy). All animal experiments were carried out in strict accordance with the Italian laws (DLvo 26/2014 and following additions) and were approved by the institutional committee. (6)

For the subcutaneous xenograft study, U937 cells were transduced with GFP-tagged scramble and SIRT6 shRNA. Next 0.2 x 10^6 cells (in 100 µl PBS) were injected subcutaneously in the right flank of mice. Following detection of tumor (~2 weeks after the injection), 20 tumor-bearing mice in each group were randomly assigned to receive either 3 mg/kg of doxorubicin administered intraperitoneally (at day 1 and then once more at 4-day interval) or vehicle control. Tumor volume was measured by caliper at day 20th and 30th post-tumor injection, with the following formula: (length x width2) / 2. (7)

For induction of acute leukemia, 1×10^6 HL-60 cells (scramble and SIRT6 shRNA transduced) were injected intravenously through the lateral tail vein in non-irradiated mice. After tumor engraftment, defined by means of percentage of human CD45+ cells in peripheral blood, 20 AML-bearing mice in each group were randomly assigned to receive either 1.5mg/kg of DNR administered intraperitoneally, for 3 days, or vehicle control. Human cell engraftment in the peripheral blood from tail vein was investigated by flow cytometry analyses at 35 and 45 days after transplant. The phenotype of human cells in NSG mice was evaluated using the following anti-human antibodies: anti-CD15-FITC (80H5), -CD13-PeCy7 (IMMU 103.44), -CD45-APC (J.33), -CD33-APC-Cy7 (D3HL60.251) from Beckman-Coulter (Irving, TX, USA) and anti-mouse CD45-PE (30-F11) from BD Biosciences to exclude murine cells contamination. Cell suspensions were evaluated by a FACSCalibur (BD Biosciences) using analysis gates designed to exclude dead cells, platelets and debris. Percentages of stained cells were determined and compared to appropriate negative controls. Seven-aminoactinomycin D (7AAD) from Sigma-Aldrich was used to enumerate viable, apoptotic and dead cells.

Cell Viability Assay

Cell viability was assessed by using CellTiter 96 AQueous One Solution Cell Proliferation Assay (Promega Corporation, Madison, WI, USA), as previously described.(1, 7)

Cell cycle analysis

For cell cycle analysis, cells were re-suspended in a buffer containing 0.1% Na citrate, 0.1% Triton-X, and 50 μg/ml propodium iodide. Thereafter, the isolated cell nuclei were analyzed by flow cytometry using a FACS Calibur (Becton Dickinson, Milan, Italy).

Real-time quantitative PCR

Peripheral blood (PB) and blood marrow (BM) samples were collected from 200 patients with newly diagnosed AML at Hematology Unit of IRCCS-AOU San Martino Hospital (Genoa, Italy) between September 2009 and December 2014 during routine diagnostic assessments. Total RNA was extracted

using RNeasy Mini Kit (Qiagen, Hilden, Germany). The purity and concentration of the total RNA was determined by a Nanodrop spectrophotometer (Labtech). The ratios of absorption (260 nm/280 nm) of all samples were between 1.8 and 2.0. cDNA was synthesized from 500 ng of total RNA with oligo(dT) primers using the High Capacity cDNA Reverse Transcriptase Kit (Invitrogen, Life Technologies, Carlsbad, CA) according to the manufacturer`s instructions. To evaluate the expression levels of listed genes, RT-PCR was performed using SYBR green PCR Master Mix (Applied Biosystems, CA) after optimization of the primer conditions. 20 ng of reverse-transcribed RNAs were mixed with 400 nM of specific forward and reverse primers in a final volume of 20 µl. RT-PCR was performed on an ABI Prism 7500 Sequence Detection System (Applied Biosystems, CA). Data were analyzed using the $2^{-\Delta\Delta Ct}$ method to measure the relative changes in each gene's expression compared with GAPDH expression. To determine mRNA levels by qPCR, the following primers were used: SIRT6 (forward: CCTCCTCCGCTTCCTGGTC; reverse: GTCTTACACTTGGCACATTCTTCC); GAPDH (forward CATACCAGGAAATGAGCTTGACAA; reverse AACAGCGACACCCATCCTC).

Western blotting (WB)

Whole-cell lysates and cell fractions were prepared as previously described. (7) Protein concentrations were determined by Bradford assay (Bio-Rad, CA), and equivalent amounts (40-50µg) were subjected to SDS-PAGE, transferred to PVDF membranes immunoblotted with following antibodies: anti-SIRT6 (#16486, Cell Signaling Technology, Danvers, MA, USA), anti-GAPDH (#5174, Cell Signaling Technology), anti-phospho-Histone H2A.X (Ser139) (#05-636, Millipore), anti-phospho-RPA32 (S4/S8) (#300-245, Bethyl Labs), anti-RPA32 (#2208, Cell Signaling Technology), anti-phospho-Atm (#47739, Santa Cruz Biotechnology), anti-Atm (#7230, Santa Cruz Biotechnology), anti-phospho-Chk2 (Thr68) (#16297, Santa Cruz Biotechnology), anti-RAD51 (#588-B01P, Novus Biologicals), anti-DNA-PKcs (#1552, Santa Cruz Biotechnology), anti-CtIP (#271339, Santa Cruz Biotechnology), anti-GFP (#NB600-308, Novus Biologicals) and anti-pan acetyl (#284922 Santa Cruz Biotechnology).

Band intensities were quantified by Quantity One SW software (Bio-Rad Laboratories, Inc) using standard ECL Western Blotting Detection Reagents (Thermo Fisher Scientific, IL). Densitometric analysis of western blots was carried out using ImageJ software version 1.48 (National Institute of Health).

Co-immunoprecipitation (co-IP)

Cells were lysed in IP buffer (50mM Tris-HCl [pH7.4], 150mM NaCl, 5 mM EDTA and 1%NP-40) plus phosphatase and protease inhibitors. The resulting extracts were incubated with 20 µl Protein A/G PLUS Agarose beads (Santa Cruz Biotechnology, Dallas, TX) at 4 °C for 30 min on the rocker, and then incubated with specific antibody at 4 °C overnight on the rocker. Beads were then added, and samples were left on the rocker for an additional 4 h. Lysates were then centrifuged at 800g for 5 min; the supernatant was then isolated, and the beads (bound fraction) were washed three times, boiled in 4. Laemmli SDS sample buffer (Boston BioProducts, MA), and separated using SDS-PAGE.

Immunofluorescence

10,000 cells from AML cell lines, PBMCs or cells obtained from subjects affected by AML were cytospin for 5 min at 350–500 r.p.m., fixed in 4% paraformaldehyde (PFA) for 15 min, washed three times with PBS and incubated with 0.1 M glycin for 10 min to quench PFA autofluorescence. After washing again, cells were permeabilized and stained for 90 min with a solution of 0.1% Triton X-100 and PBS plus 1% BSA containing primary antibodies at a dilution of 1:100. Cells were washed and incubated for 45 min with the appropriate secondary fluorescent antibodies. Alexa Fluor 488 anti-rabbit (#4412) and Alexa Fluor 488 anti-mouse (#4408) antibodies were purchased from Cell Signaling (Beverly, MA, United States), and Alexa Fluor 568 anti-mouse (A11061) antibody was purchased from Invitrogen (Life Technologies, Carlsbad, CA, United States). All secondary antibodies were diluted 1:400. After washes, the nuclear content was stained with DAPI reagent (Invitrogen, Life Technologies, Carlsbad, CA, United States) for 5 min and washed. The entire procedure was performed

at room temperature. The slides were then mounted with ProLong Gold Antifade reagent (Invitrogen, Life Technologies, Carlsbad, CA, United States), and images were taken using a Leica DMI3000 B microscope and analyzed with ImageJ software. Antibody to γ-H2A.X (clone JBW301) was obtained from Millipore/Merck (Darmstadt, Germany), antibody to SIRT6 (#12486) was from Cell Signaling (Beverly, MA, United States), antibody to pospho-RPA32 (S4/S8) (#4912) was from Bethyl Labs) and antibodies to RAD51 (#88572) and 53BP1 (#36823) were from Abcam (Cambridge, UK)

REFERENCES

1. Cea M, Cagnetta A, Fulciniti M, Tai YT, Hideshima T, Chauhan D, et al. Targeting NAD+ salvage pathway induces autophagy in multiple myeloma cells via mTORC1 and extracellular signal-regulated kinase (ERK1/2) inhibition. Blood. 2012 Oct 25;120(17):3519-29.

2. Irizarry RA, Hobbs B, Collin F, Beazer-Barclay YD, Antonellis KJ, Scherf U, et al. Exploration, normalization, and summaries of high density oligonucleotide array probe level data. Biostatistics. 2003 Apr;4(2):249-64.

3. Dai M, Wang P, Boyd AD, Kostov G, Athey B, Jones EG, et al. Evolving gene/transcript definitions significantly alter the interpretation of GeneChip data. Nucleic acids research. 2005 Nov 10;33(20):e175.

4. Johnson T. Bayesian method for gene detection and mapping, using a case and control design and DNA pooling. Biostatistics. 2007 Jul;8(3):546-65.

5. Subramanian A, Tamayo P, Mootha VK, Mukherjee S, Ebert BL, Gillette MA, et al. Gene set enrichment analysis: a knowledge-based approach for interpreting genome-wide expression profiles. Proceedings of the National Academy of Sciences of the United States of America. 2005 Oct 25;102(43):15545-50.

6. Allegretti M, Ricciardi MR, Licchetta R, Mirabilii S, Orecchioni S, Reggiani F, et al. The pan-class I phosphatidyl-inositol-3 kinase inhibitor NVP-BKM120 demonstrates anti-leukemic activity in acute myeloid leukemia. Scientific reports. 2015 Dec 17;5:18137.

7. Cagnetta A, Cea M, Calimeri T, Acharya C, Fulciniti M, Tai YT, et al. Intracellular NAD(+) depletion enhances bortezomib-induced anti-myeloma activity. Blood. 2013 Aug 15;122(7):1243-55.

SUPPLEMENTARY FIGURES AND LEGENDS

Figure S1

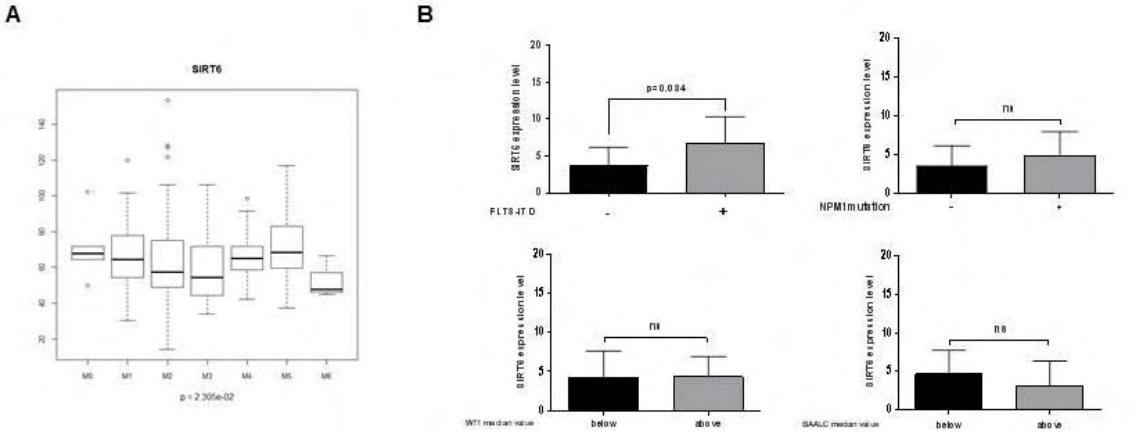

Figure S1. A) Box plot distributions of SIRT6 gene expression levels in AML patients stratified according to French-American-British (FAB) classification. SIRT6 gene expression levels (219613_s_at probe set) were obtained in purified leukemic blasts of 274 AML samples from a publicly available dataset (GSE1159) in 6 FAB classes (6 M0, 63 M1, 66 M2, 19 M3, 53 M4, 64 M5, 3 M6). Differential SIRT6 gene expression levels (natural scale) between AML groups were assessed using non-parametric Kruskal-Wallis test. **B)** SIRT6 expression was compared to genomic landscape of AML samples (n=200) collected at University of Genoa, including FLT3-ITD, NPM1 mutation WT1 overexpression and BAAL. Data are represented as mean ± SEM. ns: not significant. (Student's t test)

Figure S2

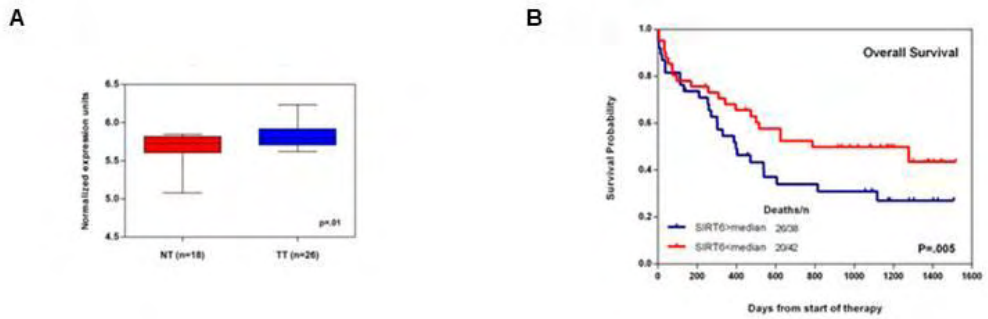

Figure S2. A) SIRT6-expression in tumor tissues (TT) of acute myeloid leukemia samples (Stirewalt et al., 2008), is compared to normal counterpart tissues (NT) (p=.01). Medians ± S.D. are represented. **B)** Kaplan-Meier plots of overall survival revealed that high SIRT6 expression conferred inferior clinical outcomes in acute myeloid leukemia (n=79),(Bullinger et al., 2004)

Figure S3

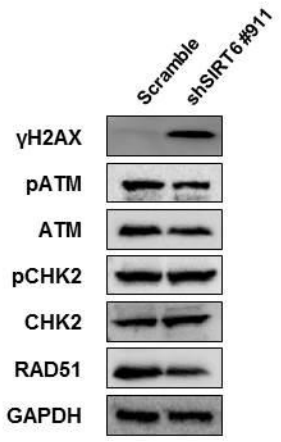

Figure S3: Representative western blots showing DDR pathway deregulation in U937 cells depleted of SIRT6 compared with control. GAPDH was used as loading control. One representative blot of two is shown.

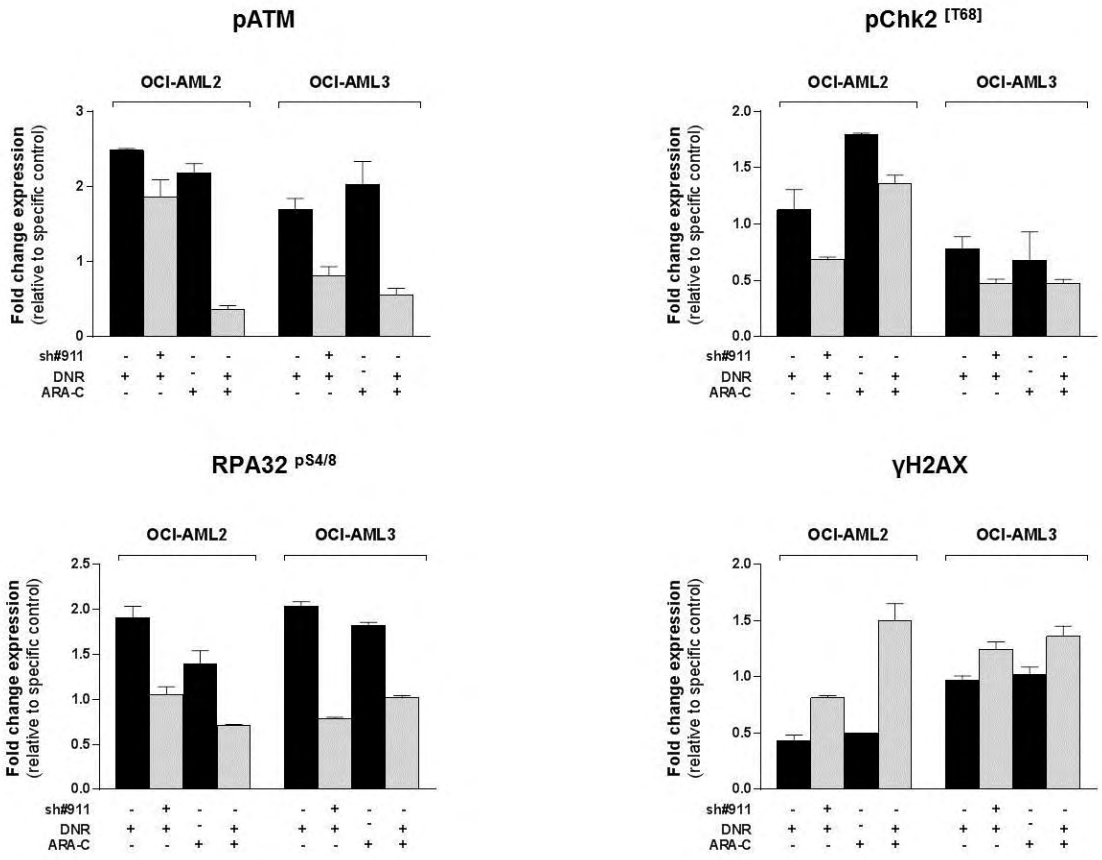

Figure S4. Densitometric analysis of Western blots from Figure 3A.

Figure S5

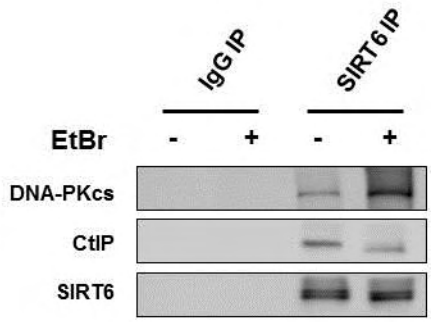

Figure S5. Endogenous SIRT6 levels in OCI-AML2 was co-immunoprecipitated in presence or not of ethidium bromide (EtBr,100 µg/ml) using an anti-SIRT6 antibody. CtIP and DNA-PKcs levels were detected by immunoblotting.

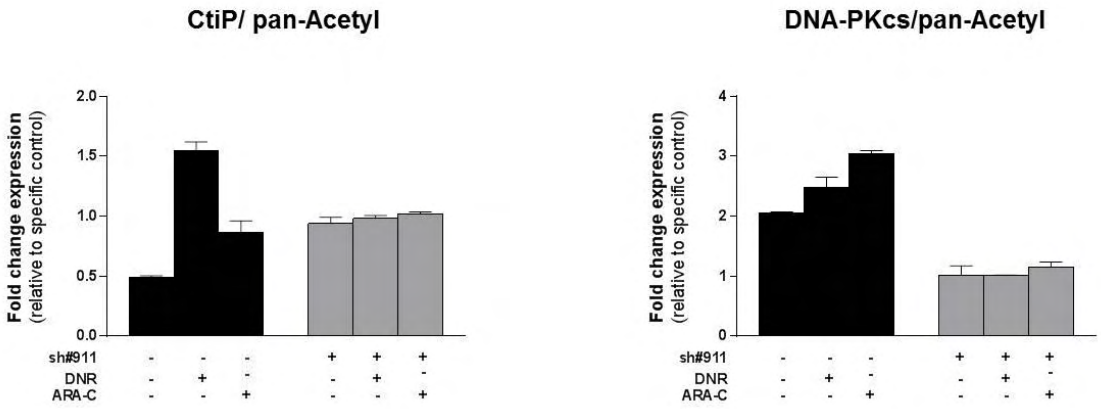

Figure S6. Densitometric analysis of Western blots from Figure 4C

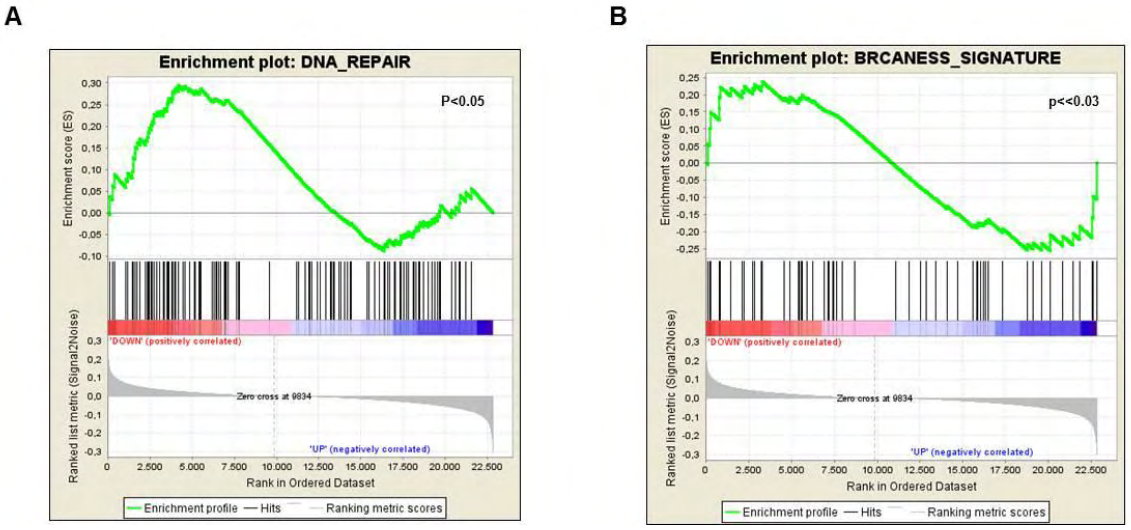

Figure S7. A, B) The pathways potentially regulated by SIRT6 were explored by GSEA in the public gene expression data set, GSE14468. AML samples were ranked by their median SIRT6 expression levels and GSEA was used to identify significantly enriched pathways. FDR: false discovery rate.

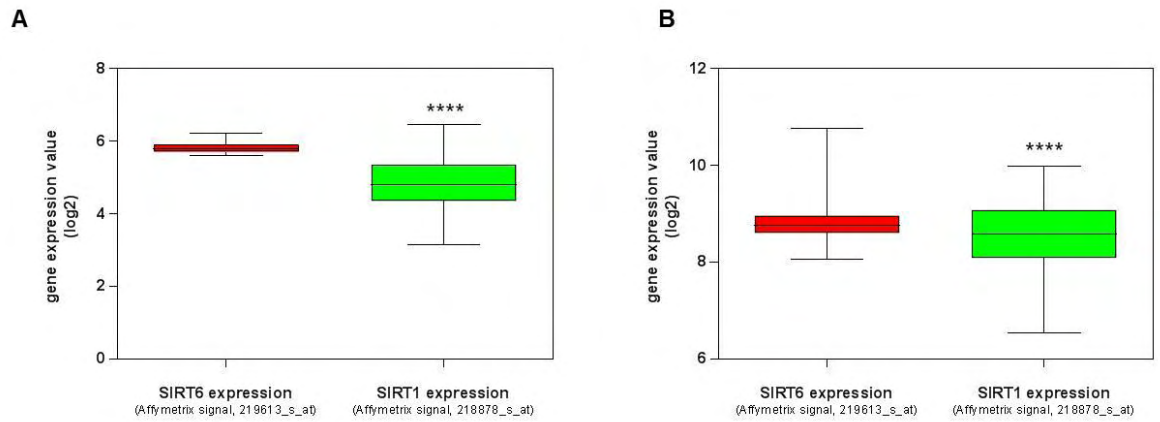

Figure S8. A,B) Expression levels (median-centered values) for SIRT1 and SIRT6 transcripts were evaluated in microarray data from AML patients (GSE37642 in **A)** and GSE9476 in **B)** using the indicated probe set. The lower and upper boundaries denote the 25th and 75th percentile, around the median value for each group.***P < 0.001 (one-way analysis of variance (ANOVA) with expression data log(2) transformed).